Mineralogical Magazine, April 2016, Vol. 80(2), pp. 239–248

The mineralogical system: Can global plots teach us something new?

MILAN RIEDER

Nanotechnology Centre VŠB-TUO, Ostrava, Czech Republic

[*Received 28 April 2015; Accepted 9 June 2015; Associate Editor: Sergey Krivovichev*]

ABSTRACT

Data based on end-member formulae of 4872 minerals (4975 entries) were subjected to numerical treatment and plotting. Most conspicuous among the findings is the hydration trend that spans the whole mineralogical system – something that may be related to the geological history of mineral formation on Earth. Interesting negative relationships were confirmed for pairs O and F, O and Cl, and Al and Si, while the O *vs.* S graph documents the dual nature of the behaviour of sulfur. Determinations of Al and Si have the potential of alarming the analyst that his phase might contain hydrogen. The dataset available also permitted the plotting of histograms that illustrate the preferred concentration distribution of individual elements throughout the mineral kingdom.

KEYWORDS: mineralogical system, information entropy, hydration trend, element relationships, element pairs and groups, hydrogen, concentration distribution of elements.

Introduction and procedures

IN a previous paper (Rieder, 2014), Shannon's (1948) information entropy ($InfEnt = \sum_i x_i \ln x_i$) was accompanied by four functions of the atomic numbers of the elements present in mineral formulae ($Qual_1 = \log \sum_i 2^{(n_i)}$, $Qual_2 = \log \sum_i x_i 2^{n_i}$, $Qual_3 = \sum_i x_i n_i$, $Qual_4 = \log \sum_i x_i n_i$; where x_i are atomic fractions of elements in the formula and n_i are their atomic numbers) and used for projecting the whole mineralogical system in 2*D*. These coordinates were calculated for 4872 end-member formulae of minerals (4975 entries, due to multiple formulae for some minerals) taken from Ciriotti's (2012) database, which defines the vintage of the data used. Questionable entries were checked against the IMA List of Minerals (Pasero, 2012) and new minerals have been added from the CNMNC newsletters (e.g. Williams *et al.*, 2014). The potential of the projections for the purpose of identification of minerals was tested, with encouraging results, and so was their possible role as a basis for plotting physical properties as a third dimension. The aim of that paper was to aid in identification of unidentified minerals or characterization of new phases from chemical data alone, and the mineral formulae extracted were modified to suit the purpose: only element totals were entered, irrespective of (1) their coordination (Al^{iv}, Al^{vi}), (2) valence (Fe^{2+}, Fe^{3+}), or (3) radical (OH, H_2O, NH_4 …). No changes in the inclusion/exclusion of elements in the database formulae were made. Also, as demanded by the calculation of *InfEnt*, all atomic quantities in the formulae were normalized to a sum of 1.0 .

All these data were stored in a matrix with 103 columns (elements) and 4975 rows (entries representing 4872 minerals). Twenty-seven columns contain only zeroes, because those elements have not yet been found in quantities sufficient to appear in an end-member formula. The matrix contains almost half-a-million data, and has served as a basis for this paper.

Standard statistical calculations were performed with the *Statistica* (Release 5, StatSoft Inc., USA). and *Statgraphics* 4.2 programs (Statpoint Technologies, Inc, USA). Additional programs

E-mail: Milan_Rieder@JHU.edu
DOI: 10.1180/minmag.2016.080.012

© *2016 The Mineralogical Society*

https://doi.org/10.1180/minmag.2016.080.012 Published online by Cambridge University Press

were written and compiled with the LF Express 73 Lahey Fortran compiler. Plots were prepared in *Origin(Pro) 7.5* (Originlab corp, USA).

Results

The basics

The first questions that come to mind are, "how many elements make up how many mineral formulae?" and "how many minerals contain a given element, element pair, or triplet?" Simple searches provided straightforward answers. Figure 1 shows that the number of elements in end-member mineral formulae ranges from one (native elements) to 16 (hellandite-(Ce)), with five-element formulae being the most numerous. Table 1 lists elements in order of decreasing frequency, Table 2 (Supplemental) shows the same for (all) 963 element pairs, and Table 3 (Supplemental) lists top 1050 element triplets from a total of 7486. Supplemental Tables 2 and 3 have been deposited with the Principal Editor of Mineralogical Magazine and are available from www.minersoc.org/pages/e_journals/dep_mat_mm.html.

The distribution of bar heights in Fig. 1 is rather similar to that in the plot of Krivovichev and Charykova (2013*a*,*b*) based on their set of 4809 minerals. In the sequence of elements in Table 1 and in a similar table of Krivovichev and Charykova (2013*a*,*b*), only the top four are identical. When plotted, the ranks define a clear 1:1 relationship with little scatter, apparently related to the inclusion/exclusion of minor components in the formulae.

Two-variable relationships

In this project, only end-member formulae were used, no intermediate solid-solutions. The initial treatment of extracted data does not make it possible to target element pairs (groups) with the same valence or in the same coordination because this information has been lost. So, even if significant correlations arise, they can result from elements playing similar roles in various senses, not just the crystal-chemical.

About 150 plots had to be seen before patterns began to emerge. In quite a few of them, the two elements plotted cannot conceivably compete for any similar crystal-chemical role, such as Na *vs.* Al, Mn *vs.* Si, or Na *vs.* O. The corresponding correlation coefficients are very low, and the plots offer no visible hints. Then there are promising plots, and plots indicating clearly visible relationships. However, the points in those plots represent all minerals containing the elements involved, so if an optically visible relationship based on one mineral group is being obscured by points from another, we would not be able to recognize that. Perhaps they could be differentiated if an additional variable were available.

One promising function for the purpose is the information entropy (*InfEnt*). Generally, the simpler the stoichiometry of a compound, the lower its *InfEnt*. It seems logical to expect minerals with simple stoichiometries (low *InfEnt*) to outline existing relationships between the elements better than those with complicated stoichiometries (high *InfEnt*). The mean *InfEnt* value for all 4975 entries is 1.163, and two boundaries, symmetrically disposed about 1.16, were defined at 1.09 and 1.23. They were used to separate the minerals into three groups, low-*InfEnt* (*InfEnt* $\leq$ 1.09, red points in plots), medium-*InfEnt* (1.09 < *InfEnt* $\leq$ 1.23, blue), and high-*InfEnt* (*InfEnt* > 1.23, green). This *InfEnt* stratification clarified a number of the plots.

Several formal aspects of two-variable plots should be pointed out: (1) Only points in which both coordinates are non-zero are plotted, so there are no data points along the axes themselves. This is because they might introduce element concentrations alien to the plot (the same holds for axial planes in Fig. 11). However, ice is plotted as a point of reference in several figures. (2) All plots are on the same scale, so whether the points cluster near the origin or are spread out over a larger area, that merely reflects the concentration preferences of the elements involved. (3) Constrained to $\Sigma x_i = 1.0$, atomic fractions might accentuate negative correlations due to the closure effect, but realistically, the effect should be expected only when larger atomic fractions are involved. In fact, among the plots seen, positive correlations slightly prevail over negative ones. (4) In some of the figures, the number of data plotted may seem lower than the *N* values indicate, but this is because there are many overlaps. Contour plots, which show frequency maxima as hills or ridges, served as an additional tool in formulating interpretations (none of those are shown here).

Where appropriate, straight lines were fitted by least squares, minimizing perpendicular distances between data points and the regression line. Numbers of data points (*N*) and linear correlation coefficients (*R*) are given in the plots.

The first plot presented is of Si against Al (Fig. 2), as these elements are almost restricted to a single valence state and a limited range of coordinations. All the correlations in the plot are

https://doi.org/10.1180/minmag.2016.080.012 Published online by Cambridge University Press

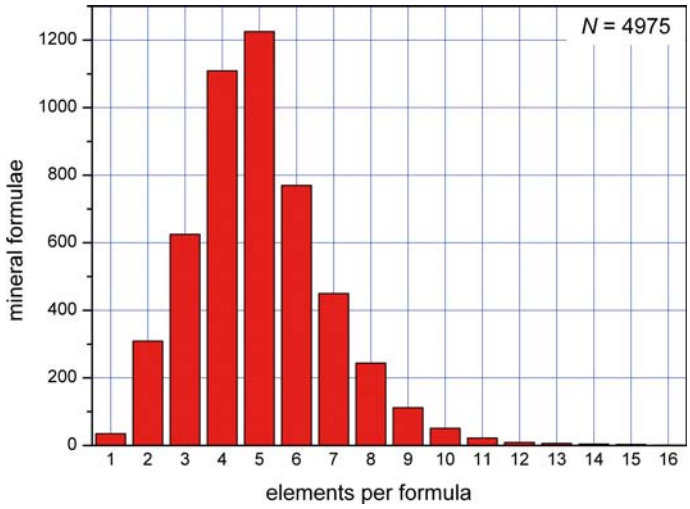


FIG. 1. Numbers of end-member formulae *vs.* the number of elements per formula.

negative, with the low-*InfEnt* group showing the tightest relationship, though based on fewest points. Interestingly, the regression line has a slope that would be displayed if the relationship were governed by the formal valences of both elements.

Negative relationships can also be seen in Figs 3 and 4, which involve elements with large ionic radii that form the anionic framework of many crystal structures. These plots are similar, and the slopes are close to 1:1 (a crystal structure can accommodate an atom of one element or the other), not a slope that is expected from their different formal valences. All correlations are negative in Fig. 4, but, curiously, the low-*InfEnt* group in Fig. 3 shows a positive correlation, albeit based on very few data (hydrous phosphates, arsenates and sulfates).

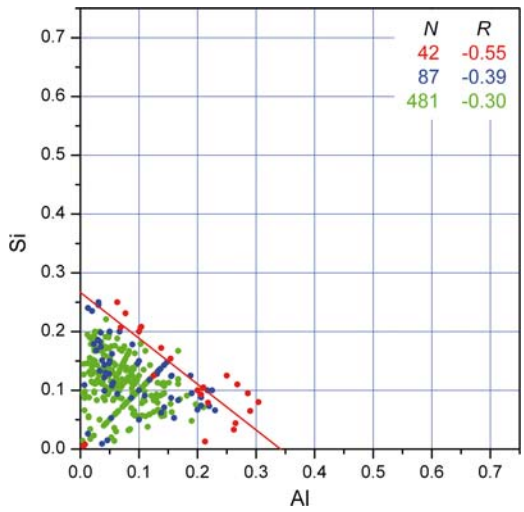


FIG. 2. Silicon *vs.* aluminium plot for 610 formulae. The low-*InfEnt* minerals and the fitted line are shown in red. Medium and high-*InfEnt* are shown in blue and green, respectively, *N* represents number of data, *R* is the linear correlation coefficient (same in all figures).

The most frequent element pair among the 4975 formulae is H and O (see Supplemental Table 2), and it exhibits a highly significant negative relationship with a slope of about –1:2 (Fig. 5). One atom of oxygen certainly does not play the same crystal-chemical role as two atoms of hydrogen, and the plot is clearly immune to any influence from coordination or valence. However, identifying minerals in the cluster, ice in particular, hints at a different cause, and the histogram showing the most frequent atomic fractions of oxygen in minerals containing no hydrogen offers further support. The pattern shown here would result if anhydrous minerals were at the starting point of a hydration trend, in the course of which various proportions of groups H_2O, (OH), or (O, OH) were being added. Accordingly, points representing minerals with an atomic fraction of oxygen corresponding to the maximum on the histogram would be moving towards the mineral ice, that is, along the main trend visible in Fig. 5. The concept of mineral evolution (Hazen *et al.*, 2008; Hazen and Ferry, 2010) makes it plain that anhydrous phases preceded hydrous phases in the Earth's history, but whether the horizontal coordinates of points in Fig. 5 have any simple relationship to the geological

https://doi.org/10.1180/minmag.2016.080.012 Published online by Cambridge University Press

TABLE 1. Seventy-six elements listed in order of decreasing frequency. Elements not present in any formulae (atomic numbers in parentheses): He (2), Ne (10), Ar (18), Kr (36), Tc (43), Xe (54), Pm (61), Eu (63), Tb (65), Po (84), At (85), Rn (86), Fr (87), Ra (88), Ac (89), Pa (91), and all those with $Z > 92$.

Element	At. no.	Minerals
O	8	4046
H	1	2844
Si	14	1472
Ca	20	1332
Fe	26	1288
Al	13	1097
S	16	1061
Na	11	1006
Mg	12	778
Cu	29	675
Mn	25	633
As	33	611
P	15	598
Pb	82	516
K	19	504
F	9	425
C	6	400
Cl	17	368
Ti	22	360
Zn	30	293
Sb	51	282
B	5	272
U	92	259
Ba	56	243
Bi	83	225
V	23	212
Ce	58	212
Ni	28	178
Nb	41	175
Ag	47	173
Te	52	168
Sr	38	150
Y	39	150
Se	34	125
Zr	40	124
Be	4	122
Li	3	121
La	57	119
Cr	24	100
Sn	50	98
N	7	97
Hg	80	92
Nd	60	79
Ta	73	76
Co	27	74
Pd	46	74
Mo	42	59
Tl	81	57
Th	90	49
Pt	78	45
W	74	40
Ge	32	31
Au	79	31
Ir	77	28
Cd	48	26
I	53	26
Rh	45	20
Cs	55	18
Br	35	16
Ru	44	16
Sc	21	15
In	49	13
Os	76	11
Gd	64	9
Dy	66	9
Yb	70	9
Ga	31	7
Sm	62	7
Pr	59	6
Er	68	6
Rb	37	3
Lu	71	3
Ho	67	2
Tm	69	2
Re	75	2
Hf	72	1

(continued)

TABLE 1. (*contd.*)

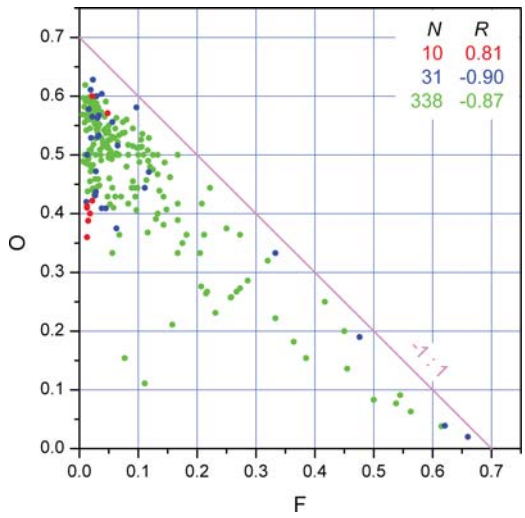


FIG. 3. Oxygen *vs.* fluorine plot for 379 minerals. Two red points at upper left are bobdownsite and stronadelphite. The arbitrarily positioned magenta line illustrates the –1:1 slope.

https://doi.org/10.1180/minmag.2016.080.012 Published online by Cambridge University Press

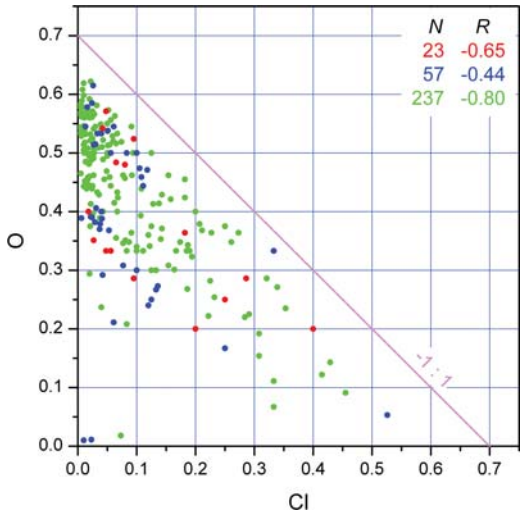


FIG. 4. Oxygen *vs.* chlorine plot for 317 minerals.

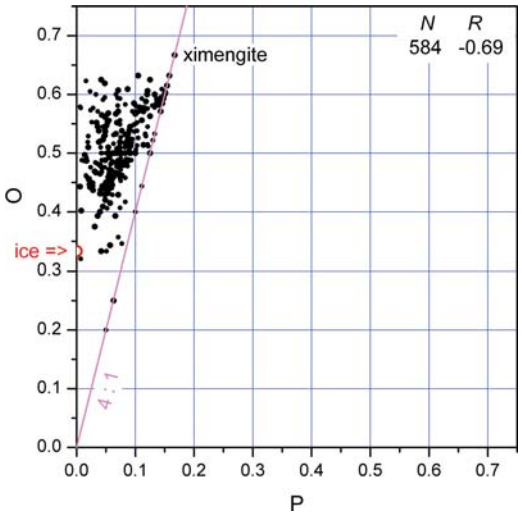


FIG. 6. Oxygen *vs.* phosphorus plot for 584 minerals.

age of those minerals (or their geologically oldest known occurrences) remains to be seen.

The following three figures offer an insight into analogies and differences between phosphates (Fig. 6), sulfates/sulfites (Fig. 7), and borates (Fig. 8). They also show that relationships between two elements are not always 'simple'. A common feature is that the magenta lines

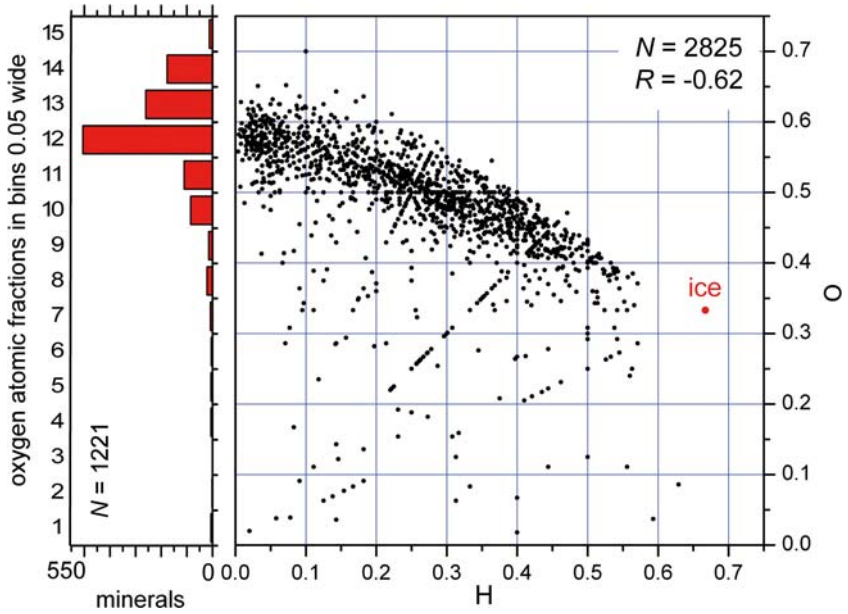


FIG. 5. Oxygen *vs.* hydrogen plot (right) combined with a frequency histogram for oxygen in minerals containing no hydrogen (left). Crucial for the interpretation of this figure, the mineral ice is shown in red. Chains of points emanating from the origin and falling on lines with slopes 2:1, 1:1, and 1:2 are due to formulae containing different proportions of groups (OOH), (OH), and H_2O, respectively.

https://doi.org/10.1180/minmag.2016.080.012 Published online by Cambridge University Press

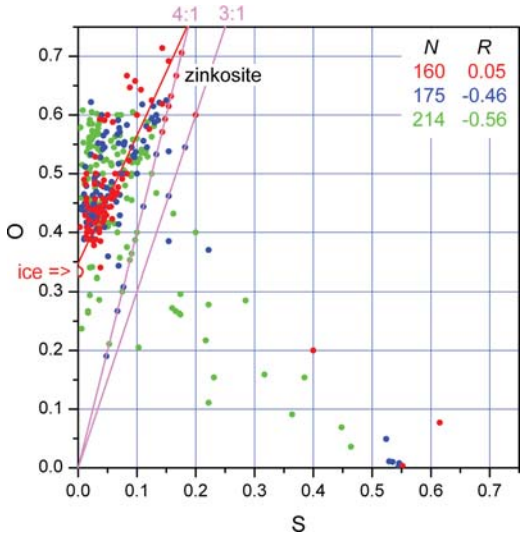


FIG. 7. Oxygen *vs.* sulfur plot for 549 minerals. The red line was fitted to red points plotting above the 3:1 magenta line (N = 156, R = 0.88).

illustrating the generally expected oxyanions are only sparsely populated (though with numerous overlaps), while many points lie above such lines. If the formulae contain additional radicals such as CO_3 or H_2O, the total number of oxygen atoms increases, thereby shifting the points upwards. Interestingly, these points are not distributed randomly, but congregate in elongated clusters, all of which point towards ice (H_2O) at their lower end. The upper end for the phosphates is either ximengite [$Bi(PO_4)$] or some of the minerals on the magenta line at O ≈ 0.6, and zinkosite [$Zn(SO_4)$] in the sulfates. Unlike these two cases, diomignite [$Li_2B_4O_7$] appears to be the upper extreme for the borates, even though it plots below the 3:1 line (its O:B ratio is 1.75:1) rather than above it. Ximengite, zinkosite, or diomignite contain no hydrogen, and so the hydration trend makes itself felt not only in Fig. 5, but in these three plots as well. Additional oxyanions present in the formulae of these mineral groups are probably responsible for the rest of the scatter, but their role appears to be subordinate.

Another interesting point concerns the bottom section of Fig. 7, below the 3:1 magenta line. The distribution of points there resembles the F *vs.* O and Cl *vs.* O plots, consistent with these points corresponding to minerals with anionic sulfur. The dense scatter of points above the 3:1 line and the negatively sloped tail at low O/S ratio thus demonstrate the two geochemical 'lives' of sulfur, as sulfide (valence = –2) in primary minerals and as oxidized salts (valence usually = +6) in secondary minerals.

Among the element pairs plotted, there are two with consistently negative correlations, H *vs.* Al and H *vs.* Si (Figs 9, 10). The vertical spread they exhibit may have been bloated by the hydration trend, and they seem to have little unexpected to say, but both regression lines have a nearly identical vertical intercept. So, hydrogen was plotted as a function of Al and Si (Fig. 11) and a plane fitted (red intercepts).

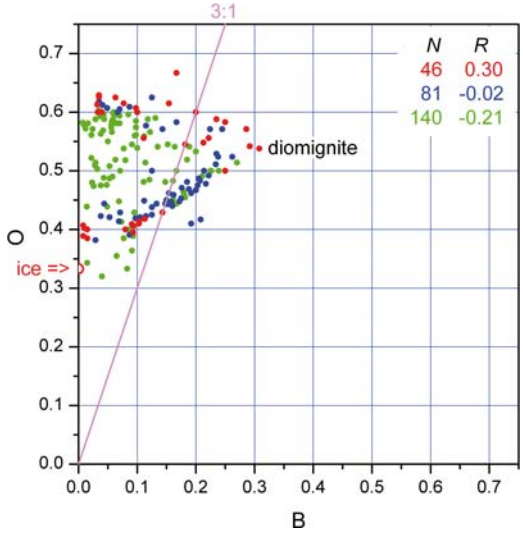


FIG. 8. Oxygen *vs.* boron plot for 267 minerals.

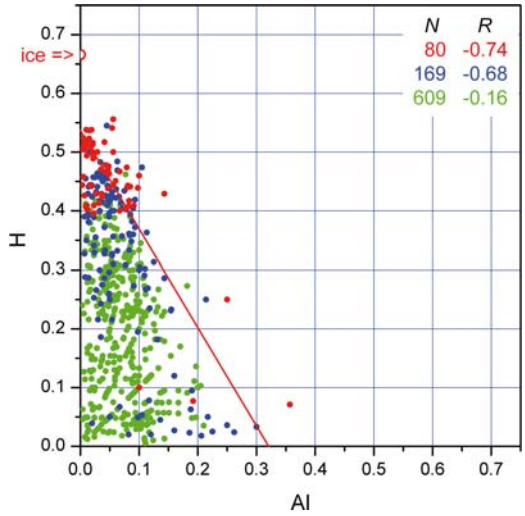


FIG. 9. Hydrogen *vs.* aluminium plot for 858 minerals.

https://doi.org/10.1180/minmag.2016.080.012 Published online by Cambridge University Press

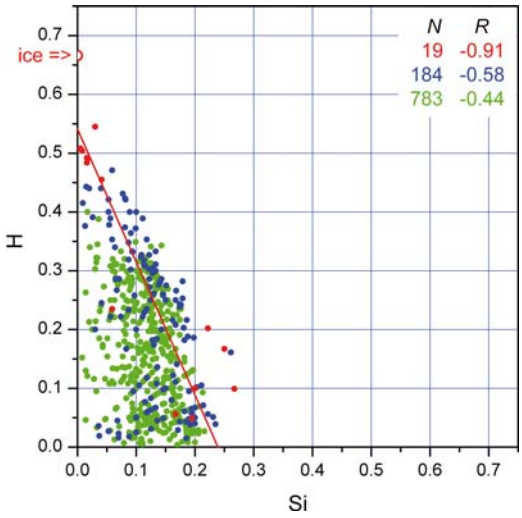


FIG. 10. Hydrogen *vs.* silicon plot for 986 minerals.

This is the 12th most frequent element triplet (see Supplemental Table 3), and the equation $H = a{\cdot}Al + b{\cdot}Si + c$ has the coefficients $a = -0.88(10)$, $b = -1.54(11)$, $c = 0.39(2)$. All the coefficients are significant on the highest level (0.0000).

Such a relationship could be valuable to those who analyse aluminosilicates using a microprobe, by sending a signal that their phase might contain hydrogen. However, the quantity of H calculated from the equation should serve as a rough indication rather than an estimate; for the latter, some fine-tuning of the relationship would be needed first.

Some points in Fig. 11 plot beyond the Loewenstein (1954) Al:Si = 1:1 limiting line, but is it not possible to say whether any of them violate the rule. The aluminium plotted here is a total for all coordinations, whereas the Loewenstein rule concerns tetrahedral aluminium only.

The populations on which Figs 2 and 11 are based partly overlap, but the regression intercepts on Al and Si axes in both figures are similar, although obtained by different procedures. In Fig. 2, the regression line is just for the low-*InfEnt* minerals containing Al and Si, whereas data in Fig. 11 were not *InfEnt*-stratified, and the intercepts are a product of extrapolating a 3*D* relationship to zero hydrogen. The Al intercepts are quite close (0.27 and 0.26, respectively), but there

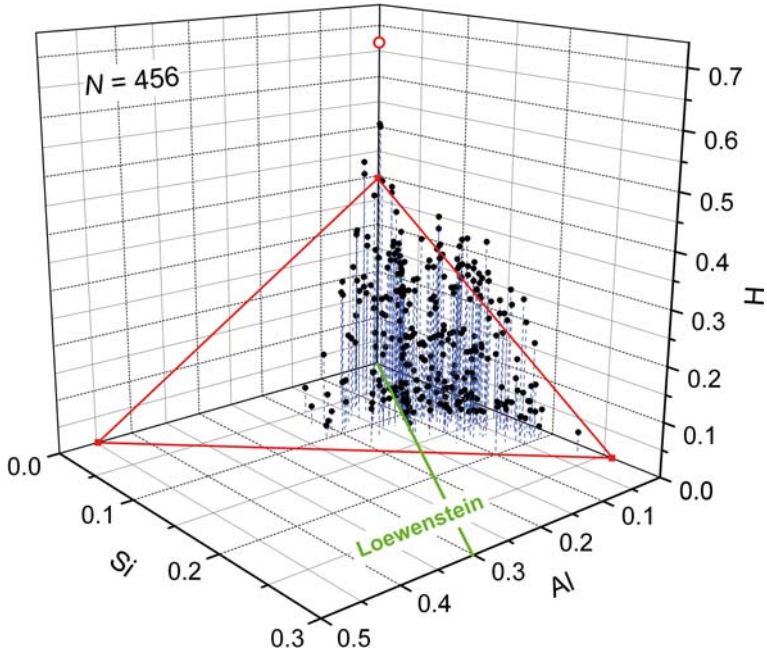


FIG. 11. Hydrogen as a function of aluminium and silicon. The hollow red circle shows the atomic fraction of hydrogen in ice. Note that none of the data plotted in Figs 9 and 10 have been included here. The Loewenstein (1954) Si:Al = 1:1 line is shown for comparison.

https://doi.org/10.1180/minmag.2016.080.012 Published online by Cambridge University Press

TABLE 4. Seven element pairs with the highest positive correlation coefficients.

Elements	Ti and Nb	Ta and Nb	P and Fe	As and Sb	Ca and K	Na and K	Mn and Fe
R	0.79	0.68	0.65	0.61	0.45	0.41	0.37
N	88	53	234	89	184	237	284

is a larger difference between the Si intercepts (0.34 and 0.45, respectively), probably due to the void section of Fig. 11 across which the regression extrapolates. Such a similarity speaks in favour of employing the *InfEnt* as a discriminating function.

Two-variable positive relationships

It is a paradox that positive correlations in element pairs only have a limited value. The chief reason is that it is difficult to differentiate between elements associated by virtue of their crystal-chemical similarities (ionic radius, valence, affinity to other elements in the compound) and elements essentially unrelated but simultaneously present in the bulk composition of a mineral-forming system. Seven pairs with the highest positive correlation coefficients (all highly significant), illustrate the point (Table 4). Most of these pairs are of elements which are crystal-chemically similar, and are either from the same group or from neighbouring groups of the Periodic Table. An exception is the Fe-P pair, which represents an anomalously high number of phosphate minerals containing Fe.

Coupled relationships?

It is tempting to explore the wealth of data available for possible symptoms of coupled substitutions, but the nature of the data (end-member formulae, element totals only, no valence information) makes it a tall order. The crucial problem is how to define the variables to be used. For example, aluminium and silicon participating in the plagioclase Na + Si ↔ Ca + Al exchange should be separate from the inert $AlSi_2$ also present in both end-member formulae, but there is no way of differentiating one from the other if only totals are available. Besides, the sets of inert elements will differ from one mineral group to another. However, all such exchanges can only proceed to the extent allowed by the smaller quantity in each pair, so plotting 2·(Na=Si) *vs.* 2·(Ca=Al) should stand a better chance. Generally, irrespective of what is plotted, when interpreting the results, a positive correlation between the variables rules out a functional mechanism, whereas a negative relationship keeps the possibility on the table.

A number of potential coupled relationships have been tested, but the results are not encouraging, only four may be hopeful. The Si *vs.* Al=H plot has enough data (456), but a prohibitive scatter resulting in a poor correlation (R = –0.34), so a comparison with the Si *vs.* Al plot (Fig. 2) is inconclusive. The plot of P *vs.* Si=H has too few data (17) and an unimpressive correlation (–0.38), as does the Na=Ti *vs.* Ca=Al plot (*N* = 6, R = –0.74). Somewhat better is the 2·(Ag=Sb) *vs.* 2·Pb plot (Fig. 12) even though its slope is gentler than the anticipated –1:1. However, sulfosalts may contain additional inert Pb, not due to this substitution, which would be impossible to distinguish and which would shift the points to the right, thus yielding a plot like we are seeing here.

In addition to the trends of the general type seen above, some coupled relationships may become

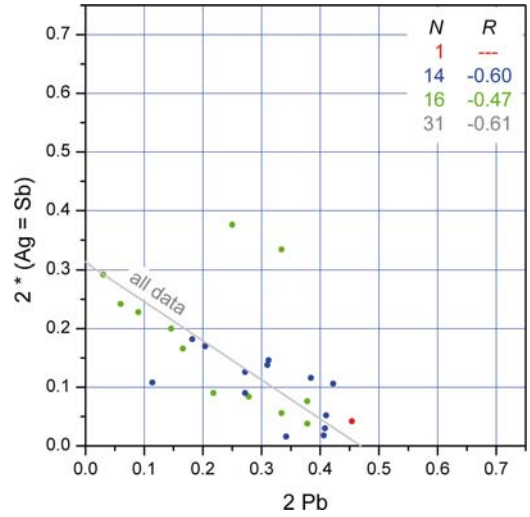


FIG. 12. A possible coupled relationship: 2·(Ag=Sb) *vs.* 2·Pb. The notation 'Ag=Sb' means 'Ag or Sb, whichever is smaller'.

https://doi.org/10.1180/minmag.2016.080.012 Published online by Cambridge University Press

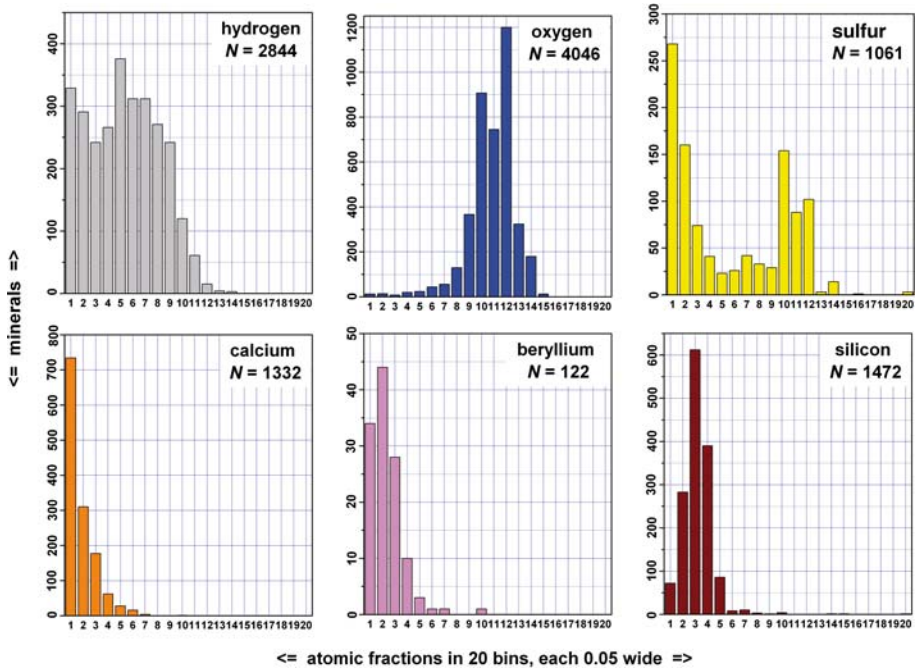


FIG. 13. Concentration distribution for six characteristic elements. The vertical scale of each plot has been adjusted to show maximum detail.

visible if restrictions are placed on element valence or coordination. Other relationships which result in compositional variation within a mineral group or even a single mineral species may become apparent only if non-end-member compositions from a single mineral group or species are considered.

Concentration distributions of elements

In addition to the features already discussed, plots in Figs 2–10 make it clear that the elements participating in mineral formulae tend to prefer some concentration ranges over others. For a closer look, atomic fractions of the elements were assigned to 20 bins, each 0.05 wide, covering concentrations between 0.0 (absent) and 1.0 (native elements) and yielding concentration histograms. Like the data shown in the O *vs.* H plot (Fig. 5), concentrations are immune to possible effects of unavailable valence or coordination. Unfortunately, there was considerable scatter for elements that occur in few mineral species, so histograms were only plotted for the 38 elements that occur in more than 100 minerals.

Generally, the structure seen in each histogram is a consequence of a conglomerate of causes ranging from crystal-chemical properties of the element to the geochemistry of the mineral-forming environment, so a strong diversification is not surprising. Figure 13 shows six characteristic concentration distributions. The broad and relatively undifferentiated maximum for hydrogen is one-of-a-kind, and so is the histogram for silicon. Also unique are histograms for oxygen and sulfur, even though they have an interesting feature in common by displaying maxima for R:O (R:S) equal to 1:1 and 2:3 (bins 10 and 12, respectively). This betrays a preference for simple compounds, in which both elements behave as divalent anions. Note that sulfur is one of the elements forming several native-element minerals (bin 20). A large number of elements show behaviour similar to Ca or Be, tending to make up only 0–10% of a mineral formula. These include Fe, Al, Na, Mg, Mn, K, F, Cl, Ti and a number of rarer elements.

Conclusions and perspectives

It is gratifying to see that basic information in the full mineral database has unexploited potential to both confirm known crystal-chemical and

https://doi.org/10.1180/minmag.2016.080.012 Published online by Cambridge University Press

geochemical trends and to reveal new relationships. These relationships, in turn, can elucidate the large-scale principles and mechanisms which govern the existence, occurrence, and diversity of minerals.

Multiple entries for some minerals are an indication that not all has been completely understood, so advancing research should provide better quality data enabling the relationships to better stand out. Also, some of the patterns shown here could become better defined if the system is narrowed down to selected mineral groups (e.g. the H *vs.* Al, Si plot). In the case of physical properties plotted as a function of *InfEnt* and the *Qual* functions (Rieder, 2014, fig. 4), the relationship cannot but improve if the reflectances (Stanley, 2013) could be associated with chemical analyses of the samples whose reflectance was measured rather than with end-member formulae taken from Ciriotti's (2012) database. Likewise, plotting data for element pairs with the same valence or treating data for elements confined to one coordination must result in an improvement, even if at a cost of some time-consuming effort. Last but not least, some relationships could use more data, but given that about 100 new species are being described annually, even those may be getting better with time.

Acknowledgements

It is a pleasure to acknowledge discussions with colleagues and friends who offered ideas, references, and encouragement: Ernst A.J. Burke, Joe Fanzone Jr., Tomas Georgievich Petrov, Roman Skála, and Stanislav Vrána; E.A.J.B. and S.V. have read an earlier version of the manuscript. The project was initiated in discussions with Chris Bendall (Springer Verlag GmbH), and was indirectly supported by the Springer Company. The paper benefited from thorough reviews by two anonymous reviewers.

References

Ciriotti, M.E. (2012) MinData Base (CLASS & SEARCH), List of all valid mineral species as recognized by IMA CNMNC, version 31.01.2012. [Most recent version available at http://cloud.amiminerals.it/index.php/s/c59e63ff95f9a6086d-fe5443db11b56e?path=%2FClassificazione].

Hazen, R.M. and Ferry, J.M. (2010) Mineral evolution: Mineralogy in the fourth dimension. *Elements*, **6**, 9–12.

Hazen, R.M., Papineau, D., Bleeker, W., Downs, R.T., Ferry, J.M., McCoy, T.J., Sverjensky, D.A. and Yang, H. (2008) Mineral evolution. *American Mineralogist*, **93**, 1693–1720.

Krivovichev, V.G. and Charykova, M.V. (2013*a*) Chislo mineralov razlichnykh khimicheskikh elementov: statistika 2012 goda (novyi podkhod k staroi probleme) [Numbers of minerals containing different chemical elements: Statistics of 2012 (a new approach to an old problem)]. *Zapiski Rossiiskogo mineralogicheskogo obshchestva*, **142**, 47–67.

Krivovichev, V.G. and Charykova, M.V. (2013*b*) *Klassifikatsiya mineral'nykh sistem [Classification of mineral systems]*. Izd-vo Sankt-Peterburgskogo gosudarstvennogo universiteta, Russia, 196 pp.

Loewenstein, W. (1954) The distribution of aluminum in the tetrahedra of silicates and aluminates. *American Mineralogist*, **39**, 92–96.

Pasero, M. (2012) *The New IMA list of minerals – A work in progress – Update: September 2012*. Available from http://nrmima.nrm.se/IMA_Master_List_%282012-09%29.pdf

Rieder, M. (2014) The mineralogical system: 2*D* projections and their potential in mineral identification. *European Journal of Mineralogy*, **26**, 703–710.

Shannon, C.E. (1948) A mathematical theory of communication. *Bell System Technical Journal*, **27**, 379–423 and 623–656.

Stanley, C.J. (2013) *COM Wavelength Database*. Natural History Museum, London.

Williams, P.A., Hatert, F., Pasero, M. and Mills, S.J. (2014) IMA Commission of New Minerals, Nomenclature and Classification (CNMNC) Newsletter 19 (New minerals and nomenclature modifications approved in 2014). *Mineralogical Magazine*, **78**, 165–170.

https://doi.org/10.1180/minmag.2016.080.012 Published online by Cambridge University Press